

Non-invasive Measurements for Shallow Depth Soil Exploration: Development and Application of an Electromagnetic Induction Instrument

Yu. A. Manstein, A.K. Manstein, E. Balkov, G. Panin.
Trofimuk Institute of Petroleum Geology and Geophysics
Siberian Branch of Russian Academy of Sciences
Novosibirsk, Russia
mansteinya@ipgg.nsc.ru

A. Scozzari
Institute of Information Science and Technologies
National Research Council of Italy
Pisa, Italy
a.scozzari@isti.cnr.it

Abstract— Sounding with alternating electromagnetic fields has gained a growing attention and a broad usage during the last three decades, including Frequency Domain Electromagnetic Induction (FD-EMI) sounding methods. The development of an instrument is briefly illustrated in this work, and experiences made by using frequency-domain EMI soundings for geophysical applications are shown. The contexts of environmental monitoring and archaeological research are included in the presented case studies, in order to assess the capability of the approach in such operative frameworks.

Keywords— *Electromagnetic induction, Geophysical surveys, Non-invasive techniques*

I. INTRODUCTION

The investigation of subsurface media structures with near surface geophysical methods involves a wide range of exploration techniques and application contexts. In many applications, the physical property of the medium that is studied is the distribution of its electric resistance, which is often very informative about subsurface structures. Electromagnetic methods have a special place in the stockroom of geophysical tools available for environmental, industrial and archeological investigations.

In this work, attention is focused on the usage of an electromagnetic induction (EMI) method, based on a multi-frequency sounding device specifically developed for shallow soil applications. Various examples of different applicative frameworks of this technique are given in the literature, from the most fascinating such as extraterrestrial geology [1] and Antarctic ice studies [2], to the most common environmental and archeological applications. Various examples in the literature deal with subjects like landfill monitoring [3], groundwater pollution [4], assessment of soil moisture patterns [5] and archeological prospections (e.g. in coastal areas) [6].

EMI is also described as an effective survey method for the detection of unexploded ordnance [7, 8]. Besides, EMI techniques are proposed in combination with GPR (Ground Penetrating Radar) for the search and characterization of buried objects [9, 10]. After briefly illustrating the principles of the technique, this work introduces the device which has been

developed and goes through selected case studies relating to archaeological and environmental applications.

II. MEASUREMENT PRINCIPLE

The basics of the method are illustrated in the sketch shown in Fig. 1. The main concept is to induce an electromagnetic (secondary) field in the soil, by placing a transmitter (Tx) of the primary electromagnetic field near the ground and measuring a secondary field by an electric and/or magnetic receiver (Rx) at the surface. In fact, the primary field induces an Eddy current, which in turn produces the secondary field, which is received together with the concatenated part of the primary field by mutual coupling between the transmitting and the receiving antennas (coils). It is thus necessary to reduce the contribution of the primary field to the measured signal. In fact, primary field cancellation reduces its contribution by a factor of up to 1000 times. No particular calibration practices are needed in order to make a correct use of the device, since the dominant systematic error is the zero response of the instrument (or free-air error), and it is compensated by subtracting an offset measured by raising the instrument at a standard height (e.g. 10m) above the ground.

In this context, Stanley et al. [11] showed a technique to generate site-specific calibrations between the apparent conductivity returned by the instrument and actual parameters of the soil, e.g. the moisture content, salinity and lithological features. Attention has been focused on the evaluation of the sensor response in presence of aluminum tubes, buried to accommodate neutron probes, which are used to make independent measurements of electrical properties of the soil.

The sounding factors in EMI methods are: i) the spacing between transmitting and receiving antennas, ii) the duration of the signal recorded after the cut-off of the transmitted signal (time domain factor), and iii) the transmitting signal frequency (frequency domain factor). Deeper discussion of these aspects can be found in [12].

III. THE INSTRUMENT

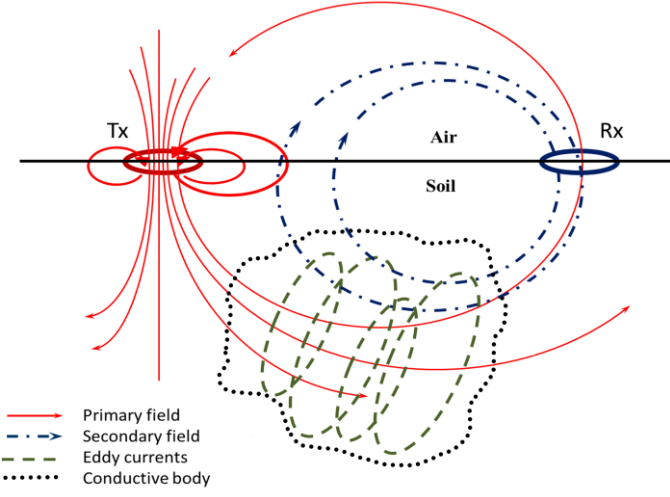


Fig. 1. Simplified representation of the basic principle of electromagnetic induction.

EMI devices are characterized by various configurations of the antennas and by different working modalities in the time domain (TEM) or frequency domain (FD-EMI) modes, the combination of which offers a wide range of possibilities. As a result, the EMI principle is embodied in a vast range of devices, which are intended to explore the Earth from the first meters to the deep mantle. In particular, the FD-EMI devices for near-surface exploration are often used for environmental studies and archeological exploration.

The electromagnetic time-domain sounding method (TEM) is based on the acquisition of the transient signal following the switch-off of a direct current flowing into the transmitting coil. This method is widely used nowadays in petroleum exploration [13], providing excellent data, thanks to the relaxation processes at deeper layers of the Earth, which are relatively slower than the shallower processes. However, in shallow Earth investigation, when the time of measurement is very short, the results of TEM are generally unstable and less appreciated for practical applications.

As shown in [9], the combination of GPR and EMI is a promising approach for an improved mapping of soil features, being the first mainly sensitive to the dielectric permittivity of the medium (and its gaps at the interface boundaries), while the second mostly depends on the electrical conductivity of the medium. A known limitation of GPR consists in the very high signal attenuation through highly conductive media, which is generally dealt with a longer wavelength, at the expense of a poorer resolution and discrimination capability.

FD-EMI has also known drawbacks and limitations, such as the limited depth of investigation in the case of hand-held devices (being a function of the distance between the antennas), and the impossibility to reconstruct cross-sections when non-conductive media are involved.

The equipment described in this paper is a portable device, intended to measure the electrical conductivity of soils to a depth of 10 m below the ground surface, for the detection of flaws, waste disposals, pipeline leakages, groundwater pollution, cavities, etc. The instrument is a 2.5 m long tool, which contains three coils corresponding to the following magnetic dipoles: a transmitter having 320 mm diameter, which is located in a dish at one end of the probe, and two receivers, which are located at different positions inside a tube on the opposite end of the transmitting dipole. An interesting discussion about minimization of mutual inductance between transmitting and receiving coils (i.e., minimization of the primary field effect) can be found in [14].

The dipole moments are mutually parallel and are perpendicular to the longitudinal axis of the probe [15]. The sounding device makes successive samplings at 14 different excitation frequencies, within the range from 2.5 KHz to 250 KHz; the sounding depth is proportional to $\sqrt{1/f}$.

A. Hardware

Signals coming from the two receiving antennas (L1 and L2) are fed to the front-end stage, consisting in a differential amplifier followed by an analog band-pass filter (see Fig. 2). Both the received signal and the primary field signal (which is captured by a dedicated current sensor) undergo a synchronous demodulation, in the classical embodiment by phase-inverting buffers and a fast analog switch.

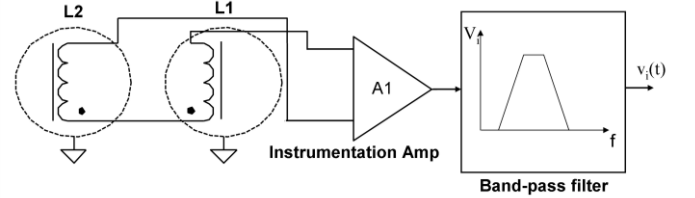


Fig. 2. Connection of the receiving antennas to the input front-end.

The two synchronous demodulators are driven by a generator that synthesizes all the transmitter excitation signals as well as the reference signals of the receivers, ensuring a stable phase relationship between them. This functionality is implemented in a Programmable Gate Array (PGA) manufactured by Atera (EPM3064).

A simplified scheme of the whole hardware is reported in Fig.3, while further details can be found in [15]. Being driven by a square signal, each multiplier is actually formed by an analog inverter and a switch, which selects between the original signal and its phase-inverted version. The two square signals $v_{R1}(t)$ and $v_{R2}(t)$ are generated in quadrature by the PGA, in order to separate the real and imaginary component of the signals $v_i(t)$ and $v_c(t)$, respectively representing the received field and the primary field. In fact, a current probe coupled with the transmitting antenna is connected to a dedicated front-end and demodulation stage, in order to provide an estimation of the amplitude and phase of the primary field, which is used by post-processing software for normalization purposes. The phase relationship between the signals $v_R(t)$ and the transmitter excitation $v_o(t)$ is set by the PGA, and their phase relationship

with the received signals is considered as constant in the absence of metal objects in the proximity of the device.

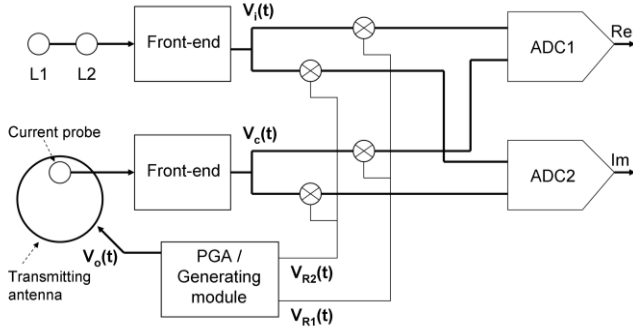


Fig. 3. Simplified block diagram of the hardware of the acquisition system.

Two multichannel converters (AD7799), one dedicated to the real component of the collected signals, the other dedicated to the imaginary part, perform a low-pass filtering (-20dB @ f=10Hz) followed by an A/D conversion with an internal 24 bit sigma-delta converter. Digital signals are then fed to the onboard control system. Details about the control system of the measuring equipment can be found in [15]. Fig. 4 shows the external appearance of the instrument.

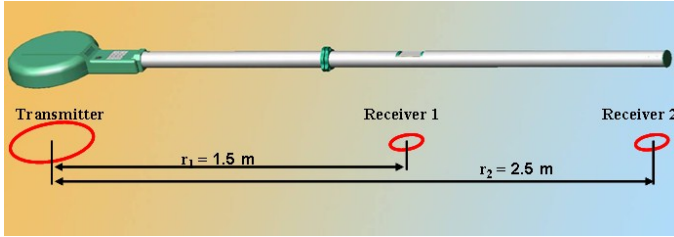


Fig. 4. External appearance of the device.

The configuration of the receiving antennas (solenoids) allows for primary field cancellation by obeying to the following relation:

$$\frac{M_1}{r_1^3} = \frac{M_2}{r_2^3}$$

where M_1 and M_2 are the magnetic moments of the receiving solenoids and r_1 , r_2 are their respective distances from the axis of the transmitting solenoid.

The main peculiarities of this device, with respect to the most common configurations seen in the literature, are the following: i) signals from the two receiving antennas are digitized after differentiation by a high stability analog stage; voiding direct digital conversion of the two received signals eliminates issues of matching between the two channels; ii) the layout and the electrical configuration of the 3 antennas allows for high rejection (up to a factor 1000, depending on the frequency) of the primary field; iii) data can be visualized in the form of maps of apparent conductivity or raw signals (quadrature, in-phase, or module of normalized received currents); iv) the transmitting antenna is made resonant at the transmitted frequency by an array of switched capacitors, at the benefit of a higher efficiency than the one obtained by direct

digital synthesis of the transmitted waveform applied to a non-adapted antenna.

B. Software

The methodology of near-surface EMI surveys includes linear and areal exploration approaches. The first class of approaches gives vertical cross sections (i.e., EMI sounding) and/or linear diagrams (i.e., EMI profiling). Instead, the areal exploration results can be presented as maps and 3D pictures, still giving the possibility to extract particular cross-sections or viewpoints.

The potentiality of lightweight portable devices of today (i.e. tablets, smartphones etc.) permits the representation of data while the survey is in action. In particular, software specifically developed for devices based on the Android operating system is now available.

Two screenshots of the software realized for Android devices are shown in Fig. 5 and Fig. 6, showing respectively the survey design and geo-location functionality and one example of elaborated output.

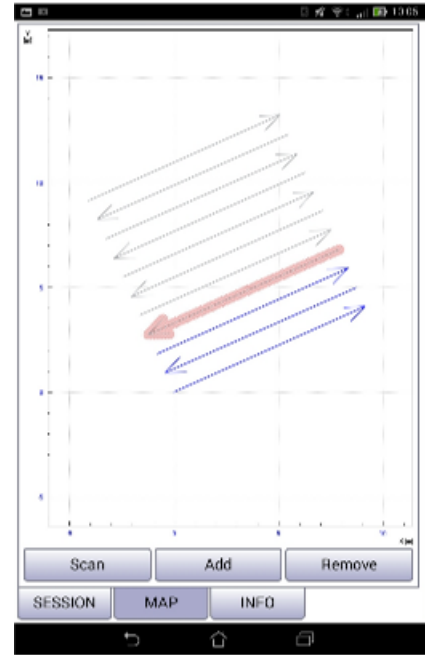


Fig. 5. Screenshot of the Android software. Layout of the survey and geo-location.

In addition to the mere profiling, the capability to build immediate 3D representations and cross-sections during the measurement campaign enhances the possibility to make interpretations and combine the results with other methods of investigation, upon decision taken on the field, while the survey is in action.

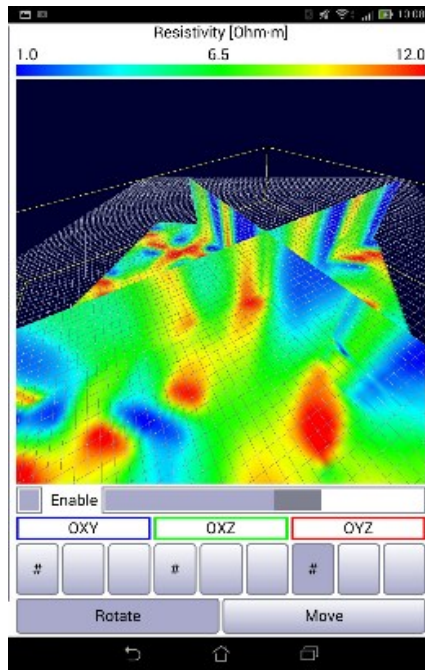


Fig. 6. Screenshot of the Android software. 3D data representation.

IV. CASE STUDIES

Three examples are given here as selected case studies. Results are shown in order to assess the potentiality of this non-invasive electromagnetic technique. Deeper details and comments about the specific applications can be found in the cited literature, being outside the scope of this paper.

Fig. 7 shows results obtained in a contaminated site, where in the late -80s a relevant quantity of expired pesticides were buried in a 5 m-deep pit, covered by loamy soil and concrete. Two volumes of anomalous low resistivity have been found, at opposite sides of the cross-section shown. Such anomalies have been confirmed by an electrical resistivity tomography survey (ERT) and by soil sampling with subsequent chemical measurements [4].

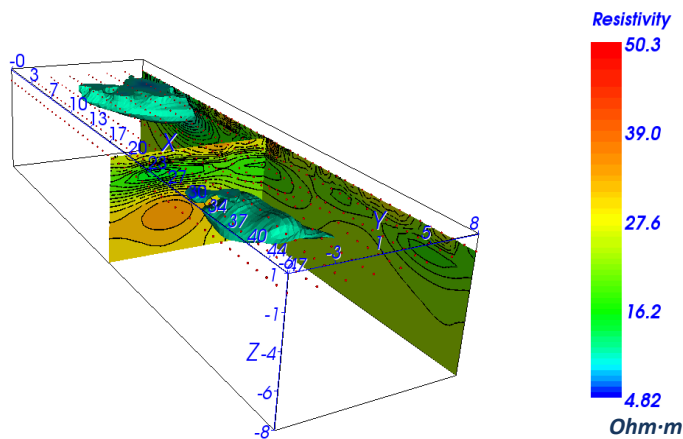


Fig. 7. 3D representation of the results obtained in the pesticide contamination case study.

Fig. 8 presents the EMI mapping of an area pertaining an abandoned zinc factory. The drainage from this site consists of a mixture of copper, silver and other water-soluble sulphates. Negative anomalies in the measurement of resistivity are indicative of groundwater contamination.

Also in this case the combination with ERT permitted to identify zones of particular pollution in the aquifer, individuating the depth of the layers reached by the plume of contaminant [4].

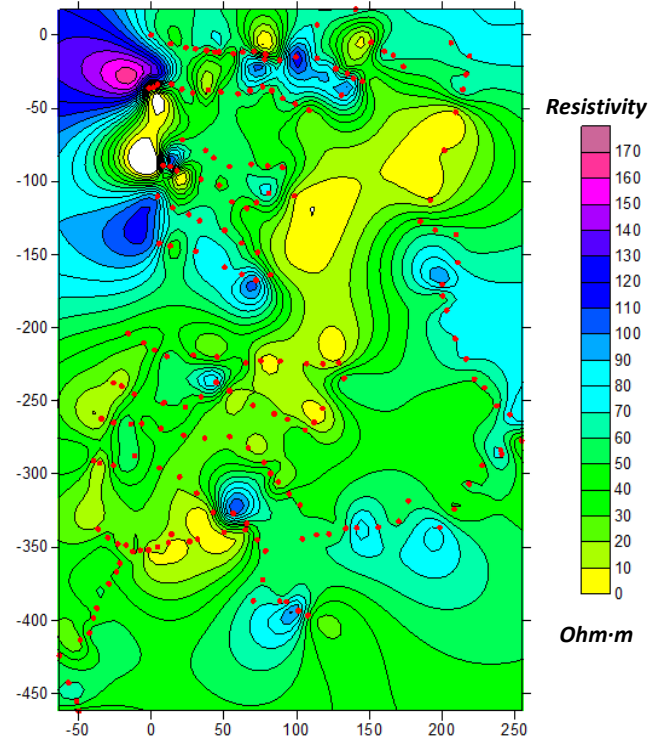


Fig. 8. Drainage area of the zinc factory. Resistivity map of the investigated site.

Finally, Fig. 9 shows results of the measurement campaign over a mound in western Siberia anterior to 1000 B.C., characterizing nomadic civilizations of the time. Patterns in the 3D representation provide information about the buried structure, in particular the 'C-shaped' positive anomaly indicates the presence of some sort of cavity, which is clearly identified.

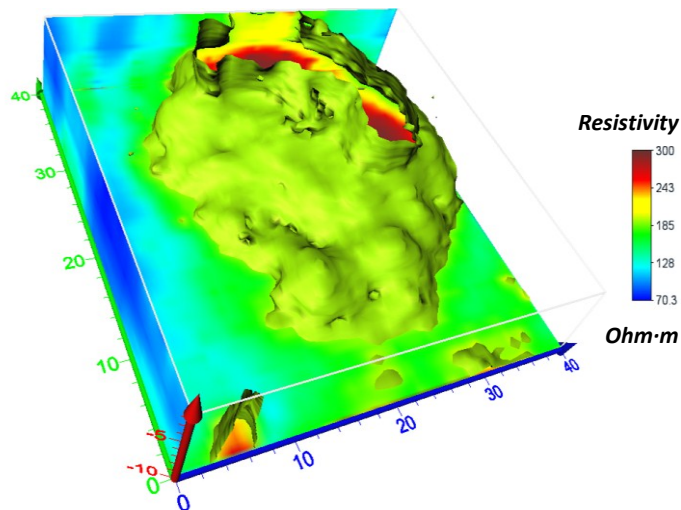


Fig. 9. 3D representation of an ancient mound. A 'C-shaped' cavity is clearly individuated.

CONCLUSIONS

This paper shows the working principle and a practical embodiment of a portable device for non-invasive shallow depth investigations by electromagnetic induction, essentially oriented to environmental and archeological applications.

After briefly discussing the main features and limitations of the FD-EMI technique, referring also to other existing systems, some selected case studies are presented.

The application examples confirm its capability to individuate buried objects, groundwater pollution and cavities in terms of anomalies in the apparent electrical conductivity of the medium. With respect to the known literature, the capability to monitor polluted sites and to reconstruct 3D patterns in archeological prospection has a particular focus in this work.

REFERENCES

- [1] Khurana K K, Kivelson M G, Russell C T, 2000 Sounding of Europa's interior using multi-frequency electromagnetic induction from a Europa orbiter. *Bulletin of the American Astronomical Society* **32** 1642
- [2] Worby A P, Griffin P W, Lytle V I, Massom R A, 1999 On the use of electromagnetic induction sounding to determine winter and spring sea ice thickness in the Antarctic. *Cold Regions Science and Technology* **29** issue 1 49-58
- [3] Jansen J, Haddad B, Fassbender W, Jurcek P, 2007 Frequency Domain Electromagnetic Induction Sounding Surveys for Landfill Site Characterization Studies. *Ground Water Monitoring & Remediation* **12** issue 4 103-109
- [4] Manstein Y, Scozzari A, 2014 Pollution detection by electromagnetic induction and electrical resistivity methods: an introductory note with case studies, from: Threats to the quality of groundwater resources: prevention and control, *Hdb Env Chem*, DOI 10.1007/698_2014_277, Springer-Verlag Berlin
- [5] Tromp-van Meerveld H. J., McDonnell J.J., 2009 Assessment of multi-frequency electromagnetic induction for determining soil moisture patterns at the hillslope scale. *Journal of Hydrology* **368** 56-67, Elsevier
- [6] Delefortrie S, Saey T, Van De Vijver E, De Smedt Philippe, Missiaen T, Demerre I, Van Meirvenne M, 2014 Frequency domain electromagnetic induction survey in the intertidal zone: Limitations of low-induction-number and depth of exploration. *Journal of Applied Geophysics*. **100** 14-22, Elsevier
- [7] Song LP, Oldenburg DW, Pasion LR, Billings SD, and Beran L, 2015 Temporal Orthogonal Projection Inversion for EMI Sensing of UXO. *IEEE Transactions on Geoscience and Remote Sensing*. **53** issue 2, 1061-1072
- [8] Shubitidze F, Fernández JP, Barrowes BE, Shamatava I, Bijamov A, O'Neill K, and Karkashadze D, 2014 The Orthonormalized Volume Magnetic Source Model for Discrimination of Unexploded Ordnance, *IEEE Transactions on Geoscience and Remote Sensing*. **52** issue 8, 4658-4670
- [9] Saey T, Delefortrie S, Verdonck L, De Smedt P, Van Meirvenne M, 2014 Integrating EMI and GPR data to enhance the three-dimensional reconstruction of a circular ditch system. *Journal of Applied Geophysics* **101** 42-50, Elsevier
- [10] Yuksel SE, Ramachandran G, Gader P, Wilson J, Ho D, and Heo G, 2008 Hierarchical methods for landmine detection with wideband electro-magnetic induction and ground penetrating radar multisensor systems. *IEEE IGARSS 2008 Conference*, vol 2 177-180
- [11] Stanley JN, Lamb DW, Irvine SE, Schneider DA, 2014 Effect of Aluminum Neutron Probe Access Tubes on the Apparent Electrical Conductivity Recorded by an Electromagnetic Soil Survey Sensor, *IEEE Geoscience and Remote Sensing Letters*. **11** issue 1, 333-336
- [12] Balkov EV, Epov MI, Manstein AK, Manstein YA, 2006 Electromagnetic induction frequency sounding: estimation of penetration depth, *Near Surface Conference 2006*, vol 4
- [13] Wilt M, Alumbaugh D, 2003 Oil field reservoir characterization and monitoring using electromagnetic geophysical techniques. *Journal of Petroleum Science and Engineering* **39** 85- 97
- [14] Reed MA and Scott WR Jr., 2013 Optimal coils with zero mutual inductance for electromagnetic induction systems. *IEEE IGARSS 2013 Conference*, 1406-1409
- [15] Manstein AK, Panin GL, Tikunov SY, 2008 A device for shallow frequency-domain electromagnetic induction sounding, *Russian Geology and Geophysics* **49** 430-436